Cancer Cell
Article

Treatment-Emergent Mutations in NAEβ Confer Resistance to the NEDD8-Activating Enzyme Inhibitor MLN4924

Michael A. Milhollen,[1] Michael P. Thomas,[1] Usha Narayanan,[1] Tary Traore,[1] Jessica Riceberg,[1] Benjamin S. Amidon,[1] Neil F. Bence,[1] Joseph B. Bolen,[1] James Brownell,[1] Lawrence R. Dick,[1] Huay-Keng Loke,[1] Alice A. McDonald,[1] Jingya Ma,[1] Mark G. Manfredi,[1] Todd B. Sells,[1] Mike D. Sintchak,[1] Xiaofeng Yang,[1] Qing Xu,[1] Erik M. Koenig,[1] James M. Gavin,[1] and Peter G. Smith[1,*]
[1]Discovery, Millennium Pharmaceuticals, Inc., Cambridge, MA 02139, USA
*Correspondence: peter_smith@h3biomedicine.com
DOI 10.1016/j.ccr.2012.02.009

SUMMARY

MLN4924 is an investigational small-molecule inhibitor of NEDD8-activating enzyme (NAE) in clinical trials for the treatment of cancer. MLN4924 is a mechanism-based inhibitor, with enzyme inhibition occurring through the formation of a tight-binding NEDD8-MLN4924 adduct. In cell and xenograft models of cancer, we identified treatment-emergent heterozygous mutations in the adenosine triphosphate binding pocket and NEDD8-binding cleft of *NAEβ* as the primary mechanism of resistance to MLN4924. Biochemical analyses of *NAEβ* mutants revealed slower rates of adduct formation and reduced adduct affinity for the mutant enzymes. A compound with tighter binding properties was able to potently inhibit mutant enzymes in cells. These data provide rationales for patient selection and the development of next-generation NAE inhibitors designed to overcome treatment-emergent *NAEβ* mutations.

INTRODUCTION

Targeting ubiquitin and ubiquitin-like protein (UBL) pathways with small molecule inhibitors is an emerging therapeutic strategy for a variety of diseases (Schulman and Harper, 2009). Of the seventeen identified UBLs, many play critical roles in the modulation of cancer cell growth and survival pathways through their control of protein homeostasis (Nalepa et al., 2006). Our efforts to inhibit enzymes that control UBL conjugation led to the identification of MLN4924, an investigational small molecule inhibitor of the NEDD8-activating enzyme (NAE; Soucy et al., 2009a). The inhibition of NAE by MLN4924 results in the inactivation of a family of E3 ubiquitin ligases, which results in DNA re-replication and inhibition of nuclear factor (NF)-κB signaling, leading to cancer cell death (Milhollen et al., 2010, 2011). MLN4924 is currently in clinical trials and has shown clinical activity in some solid tumor and hematologic malignancies (Wang et al., 2011). Therefore, we sought to define mechanisms of resistance to MLN4924 in preclinical models of cancer.

The inhibition of NAE by MLN4924 occurs through the formation of a NEDD8-MLN4924 covalent adduct resembling NEDD8-AMP, a process that requires NAE catalytic activity (Brownell et al., 2010). Importantly, the NEDD8-MLN4924 adduct is a tight binding inhibitor of NAE, and it has been proposed that the tight binding nature of the inhibitor-protein adduct is crucial for MLN4924 potency (Brownell et al., 2010). The best characterized substrates of NEDD8 conjugation are the cullin scaffold proteins of the cullin-RING ligase (CRL) complexes, which control the ubiquitination and proteasomal destruction of numerous cancer-relevant proteins (Soucy et al., 2009b; Watson et al., 2011). Thus, inhibition of NAE and NEDD8 conjugation by MLN4924 leads to the inhibition of CRL activity and perturbation of cellular protein homeostasis (Soucy et al., 2009a). The evaluation of MLN4924 in cellular and tumor xenograft studies has revealed two distinct mechanisms of action. The first is the

Significance

There are numerous examples of target-based mutations leading to treatment-emergent resistance in oncology (e.g., with imatinib). This has enabled drug discovery efforts resulting in the identification of superior and/or second-generation inhibitors. As a result of this trend, predicting and responding to resistance is critical to the full exploitation of an oncology target and to promptly meeting the needs of patients. Compelled by clinical activity of MLN4924 in acute myelogenous leukemia, we sought to preemptively define the landscape of resistance mechanisms and identified treatment-induced mutations of *NAEβ*. If resistance occurs in the clinic, these findings will accelerate our assessment of the molecular cause and provide insights into the development of second-generation NAE inhibitors.

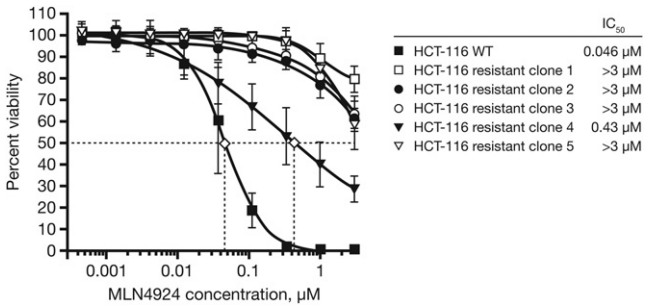

Figure 1. MLN4924-Resistant HCT-116 Clones Show Reduced Sensitivity to MLN4924

HCT-116 WT cells and resistant clones were treated with DMSO or various concentrations of MLN4924 for 96 hr, and cell viability was assessed with an ATPlite assay. Data shown are mean ± standard deviation (n = 3 experiments). See also Figure S1.

induction of DNA re-replication, DNA damage, and cell death through MLN4924-mediated dysregulation of the $CRL1^{SKP2}$ and $CRL4^{DDB1}$ substrate CDT1 (Milhollen et al., 2011). It has been shown that p53 status does not impact the induction of DNA re-replication but may make cells more prone to undergo apoptosis or senescence, depending on the appropriate genetic background (Milhollen et al., 2011; Lin et al., 2010a, 2010b). The second mechanism is the inhibition of NF-κB pathway activity in NF-κB-dependent diffuse large B cell lymphomas (DLBCL), primarily through dysregulation of $CRL1^{\beta TRCP}$-mediated turnover of phosphorylated IκBα (Milhollen et al., 2010). In addition, preclinical models of acute myelogenous leukemia (AML) are sensitive to MLN4924 inhibition in both cell lines and primary patient blasts through mechanisms related to CDT1 dysregulation, NF-κB inhibition, and induction of reactive oxygen species (Swords et al., 2010). These data highlight the therapeutic potential of MLN4924 in a diverse set of preclinical cancer models.

MLN4924 is currently undergoing phase I clinical testing in a variety of solid tumor and hematological malignancies (Wang et al., 2011). Clinical activity has been described in patients with AML with reports of 3 of 15 patients achieving a complete response on MLN4924 therapy (Wang et al., 2011). With initial signs of clinical activity with a pathway inhibitor, it is increasingly important to identify potential mediators of resistance in preclinical models that can be predictive of clinical observations (Sellers, 2011). Thus, we utilized cellular and tumor xenograft models of cancer as an approach to study acquired resistance to MLN4924.

In this report we describe the emergence of heterozygous mutations in the NAEβ (UBA3) subunit of NAE in cell lines and xenograft models of cancer following selection pressure with MLN4924. We evaluate how such mutations may reduce compound potency and present evidence in cells and xenografts regarding pathway inhibition, levels of NAEβ-bound NEDD8-MLN4924 adduct, and recovery of pathway activity following inhibition. Finally, we investigate a pan-E1 inhibitor with tighter binding properties and its ability to inhibit NEDD8 conjugation in MLN4924-resistant cells carrying a mutation in NAEβ.

Table 1. Heterozygous Mutations in *NAEβ* Detected in MLN4924-Resistant HCT-116, NCI-H460, and Calu-6 clones

Cell Line	NAEβ Status Sanger	Sequenom
HCT-116 parental	WT	WT
HCT-116.1	A171T	A171T
HCT-116.2	A171T	A171T
HCT-116.3	A171T	A171T
HCT-116.4	C324Y	C324Y
HCT-116.5	G201V	G201V
NCI-H460 parental	WT	WT
NCI-H460.1	E204K	E204K
NCI-H460.2	A171D	A171D
Calu-6 parental	WT	WT
Calu-6.1	N209K	N209K

See also Figure S2 and Tables S1, S2, and S4.

RESULTS

Clonal Selection of Tumor Cell Lines that Are Resistant to MLN4924 Show Reduced Pathway Inhibition In Vitro and Contain a Mutation in *NAEβ*

Three solid tumor cell lines (HCT-116 colorectal, NCI-H460 lung, and Calu-6 lung) that have been shown to undergo DNA re-replication in response to NAE inhibition (Soucy et al., 2009a) were chosen to study potential mechanisms of resistance to MLN4924. These cell lines have differential sensitivity to MLN4924-induced cytotoxicity, with EC_{50} values (cell viability assay) of 46, 80, and 1070 nM for HCT-116, Calu-6, and NCI-H460 cells, respectively. Cells were exposed to high concentrations of MLN4924 ($\geq EC_{90}$ concentrations) for four days, which resulted in almost-complete cell kill, and five resistant clones were obtained for HCT-116 cells. One HCT-116 clone was found to be 10-fold less sensitive to MLN4924, and four had EC_{50} values greater than 3 μM (Figure 1). Similarly, one Calu-6 clone and two NCI-H460 clones were isolated and found to have EC_{50} values of >10 μM (Figure S1 available online). The MLN4924-resistant HCT-116 cell clones remained sensitive to other chemotherapies (bortezomib, doxorubicin, and SN-38; Figure S1), suggesting that the resistance mechanism is not a shared mechanism with other agents.

To determine whether changes in the NEDD8 pathway may explain the resistance to MLN4924, cells were evaluated for changes in gene transcript levels or the presence of DNA mutations in *NAEβ*, *NAE1*, *NEDD8*, *COPS5*, or *UBC12*, the primary E2 for neddylation. No substantial changes were found in mRNA levels of neddylation pathway genes (Figure S2A). Changes were observed in mRNA levels of adenosine triphosphate (ATP)-binding cassette-transporter proteins; however, MLN4924 activity was unaffected by co-incubation with drug efflux inhibitors (Figure S2B). DNA sequencing revealed no treatment-emergent DNA mutations in *NAE1*, *UBC12*, *COPS5*, or *NEDD8*; however, heterozygous mutations in *NAEβ* were detected by Sanger sequencing in all resistant cell lines (Tables 1 and S1). These mutations were confirmed using additional mass spectrometry-based and next-generation sequencing

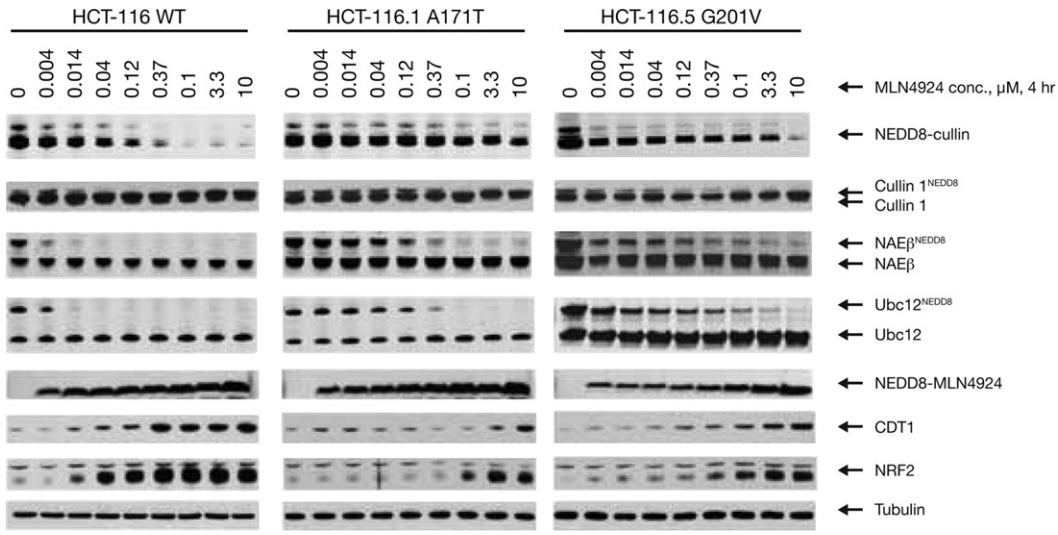

Figure 2. MLN4924-Resistant HCT-116 Clones Show Reduced NEDD8 Pathway Inhibition and Contain a Heterozygous Mutation in NAEβ
HCT-116 WT cells and resistant clones were treated with DMSO or various concentrations of MLN4924 for 4 hr. Western blots were probed for NEDD8-cullin, CUL1, NEDD8-NAEβ, NEDD8-UBC12, NEDD8-MLN4924 adduct, CDT1, NRF2, and tubulin. See also Figure S2.

methods (Table S2). The location of the mutations would be consistent with modification of MLN4924 binding in the nucleotide binding pocket (A171T and A171D) or in affecting the ability of NEDD8 to bind to NAEβ (G201V, E204K, N209K, and C324Y). Of note, a heterozygous mutation in NEDD8 (I44T) was detected in wild-type HCT-116 cells, which was maintained in the resistant clones. However, the activity of this NEDD8 mutant was identical to wild-type NEDD8 in biochemical assays (data not shown).

Pathway analysis by western blotting was performed following a 4 hr incubation of compound to assess the effect of MLN4924 on the NEDD8 pathway in the resistant clones. Two HCT-116 clones were selected for analysis (A171T and G201V), and a reduced effect of inhibition of NEDD8 conjugation to NAEβ, UBC12, and the cullin proteins was demonstrated when compared to wild-type cells (Figure 2). The reduced effect on NAE inhibition was confirmed by a reduced accumulation of two CRL substrates, NRF2 and CDT1 (Figure 2). As expected, NEDD8-MLN4924 adduct could still be detected in the resistant cell lines, since there is still one wild-type copy of NAEβ. In addition, the steady-state neddylation levels of the cullins, and specifically cullin-1 (CUL1), are similar in the three cell lines, and the inhibition of CUL1 neddylation reflects that of the total cullins (Figure 2). MLN4924 induces DNA re-replication in HCT-116 cells (Milhollen et al., 2011), yet the cell-cycle distribution of HCT-116-resistant A171T and G201V clones treated with MLN4924 is not significantly altered, consistent with their insensitivity to MLN4924 (Figure S3). Similar effects of reduced potency of MLN4924 on the neddylation pathway and CRL substrate accumulation were observed in NCI-H460 A171D clone (Figure S3). Reduced pathway inhibition was also observed in the Calu-6 N209K clone, but this was not as marked as in other resistant clones (Figure S3). These data demonstrate that in vitro-derived MLN4924-resistant cell lines contain heterozygous mutations in *NAEβ* and are, as a result, less sensitive to NAE inhibition.

HCT-116 Xenografts Become Resistant to Antitumor Effects of MLN4924, Demonstrate Reduced Pharmacodynamic Effects, and Contain Mutations in NAEβ

HCT-116 cells were grown as subcutaneous xenografts in immunocompromised rats and then subcutaneously treated with the maximum tolerated dose of MLN4924 (150 mg/kg) on a dosing schedule of days 1, 4, 8, and 11 of a 21-day therapy cycle. Importantly, this regimen was chosen as it is currently being utilized in phase I clinical studies of MLN4924 in solid and hematologic malignancies. After the first cycle of MLN4924, tumor regressions were observed that were maintained through most of the second cycle of treatment (Figure 3A). However, during cycle 3, ten of eleven tumors began to regrow, even in the presence of MLN4924 (Figure 3A). Tumors were harvested at the end of treatment and the nucleic acid sequence of *NAEβ* was analyzed. Eight of ten tumors were found to contain a heterozygous mutation at A171T of NAEβ (Figure 3A and Table S2). Interestingly, in two tumors, more than one mutation was detected (A171T/E204K and A171T/A171D/Y228H, respectively), indicating that multiple clones may emerge within a tumor population. No mutations were detected in *NAE1*, *COPS5*, or *UBC12*, and the I44T mutation within *NEDD8* was detected, consistent with cells grown in vitro.

To confirm that the tumors were now stably resistant to MLN4924, one xenograft with an A171T mutation was retransplanted into nude rats. The antitumor activity of MLN4924 was dramatically reduced compared to wild-type xenografts; one cycle of MLN4924 150 mg/kg (days 1, 4, 8, and 11) inhibited tumor growth by only 38% compared to 94% (including tumor regressions) that were observed in wild-type xenografts (Figure 3B). The A171T NAEβ mutation was still present in this resistant xenograft model as confirmed by both Sanger and Sequenom methodologies. Pharmacodynamic analysis of NEDD8 pathway inhibition by MLN4924 in HCT-116 wild-type and A171T-resistant xenografts was conducted following a single

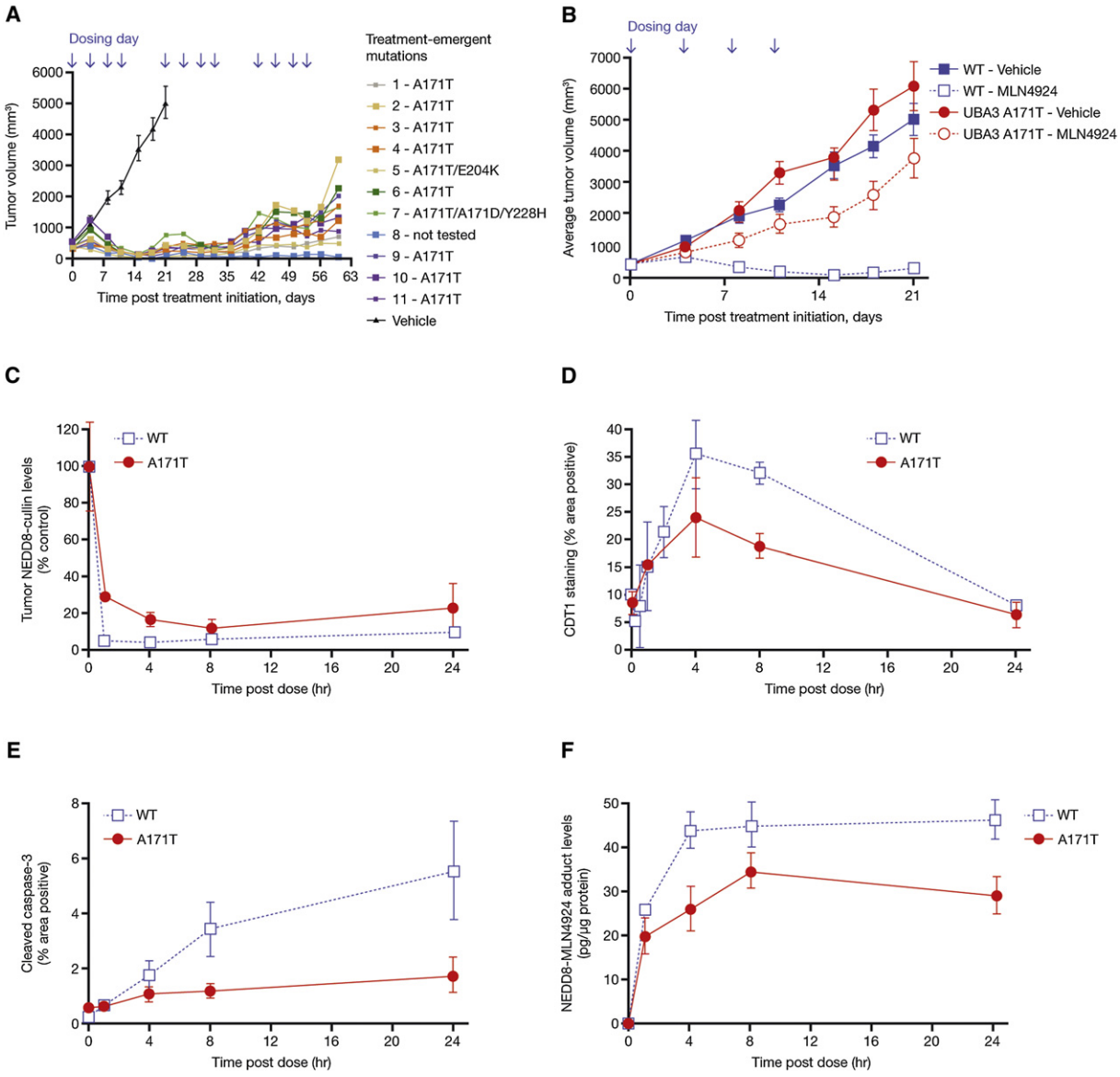

Figure 3. HCT-116 Xenograft-Bearing Nude Rats Become Refractory to MLN4924 Treatment, Contain a Heterozygous Mutation in NAEβ, and Are Resistant to Retreatment

(A) Immunocompromised nude rats bearing HCT-116 xenografts were administered MLN4924 150 mg/kg on days 1, 4, 8, and 11 of a 21-day cycle for three cycles. Tumors were harvested at the end of treatment for analysis, and the mutational status of *NAEβ* was determined. Data shown are mean ± standard error (n = 10) for vehicle group.

(B) A tumor containing an alanine 171 to threonine mutation was re-established in nude rats and treated with MLN4924 150 mg/kg on days 1, 4, 8, and 11 of a 21-day cycle. The response of WT (parental) tumors is included on the graph for comparison. Data shown are mean ± standard error (n = 10).

(C–F) Nude rats bearing HCT-116 parental or A171T xenografts were administered a single dose of 150 mg/kg MLN4924 and tumors were excised at the indicated times and measured for (C) NEDD8-cullin conjugate levels by western blotting; (D) CDT1 levels by immunohistochemistry; (E) cleaved caspase-3 levels by immunohistochemistry; and (F) NEDD8-MLN4924 adduct levels by mass spectrometry. Data shown are mean ± standard deviation (n = 3 replicates). See also Table S2 and Figure S4.

dose of MLN4924 (150 mg/kg). Maximal inhibition of NEDD8-cullin levels occurred as early as 1 hr postdose in HCT-116 wild-type xenografts compared to 8 hr postdose in the A171T-resistant model (Figures 3C and S4A). In agreement with reduced effects on NEDD8-cullin levels in HCT-116 A171T cells was a reduction in CDT1 levels (Figures 3D and S4B), apoptosis as measured by cleaved caspase-3 (Figure 3E and S4C), and NEDD8-MLN4924 adduct (Figure 3F) compared to HCT-116 wild-type xenografts. These data demonstrate that tumor xenografts treated with a clinically relevant dosing schedule can acquire resistance to MLN4924 that is associated with mutations in *NAEβ*.

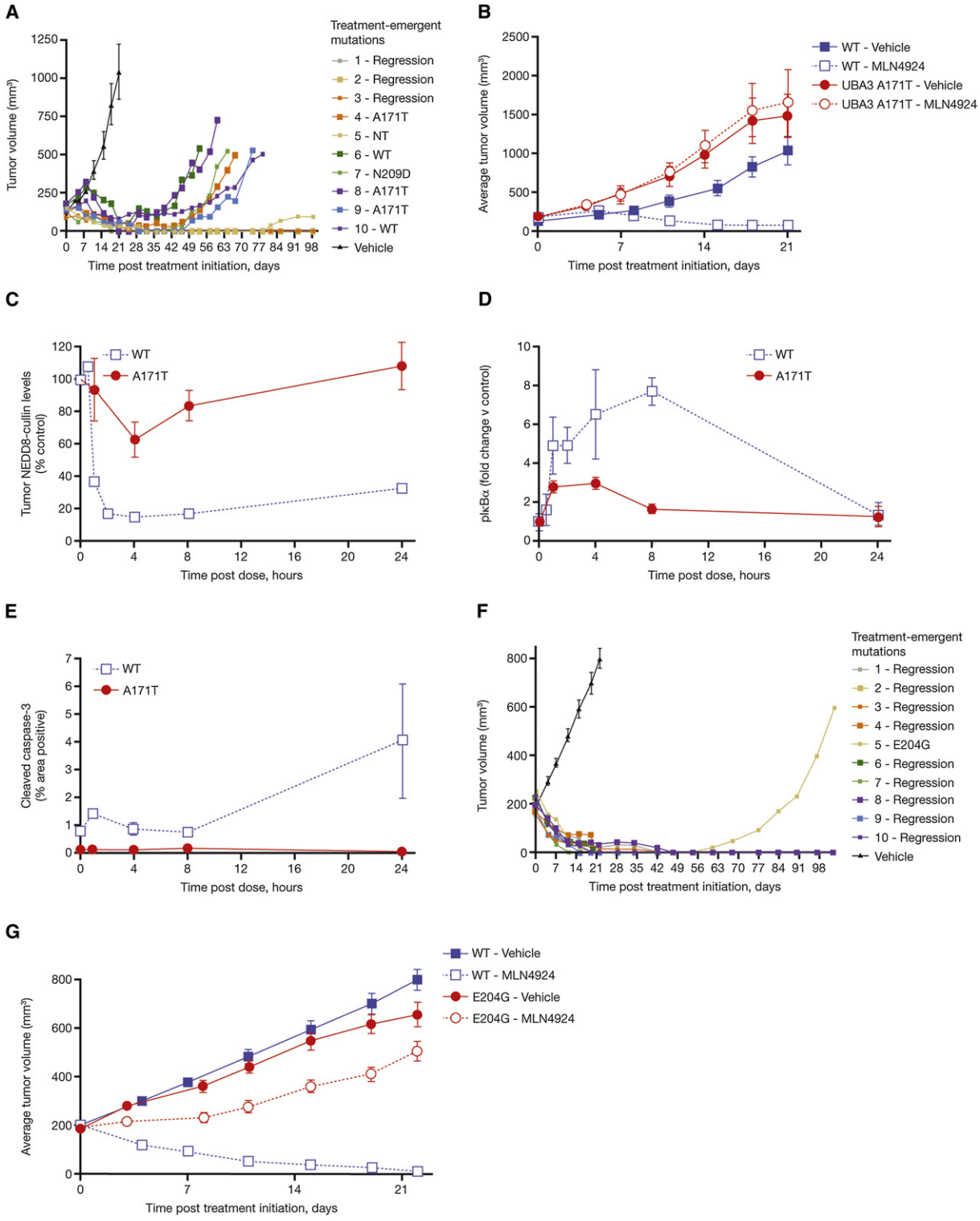

Figure 4. Acute Myelogenous Leukemia and Diffuse Large B Cell Lymphoma Xenograft-Bearing Nude Mice Become Refractory to MLN4924 Treatment, Contain a Heterozygous Mutation in NAEβ, and Are Resistant to Retreatment

(A) CB.17 SCID mice bearing THP-1 AML xenografts were administered MLN4924 90 mg/kg BID on days 1, 4, 8, 11, 15, and 18 of a 21-day cycle for up to five cycles. Tumors were harvested at the end of treatment for analysis, and the mutational status of *NAEβ* was determined. Data shown are mean ± standard error (n = 10) for vehicle group.

(B) A tumor containing an alanine 171 to threonine mutation was re-established in CB.17 SCID mice and treated with MLN4924 90 mg/kg BID on days 1, 4, 8, 11, 15, and 18 of a 21-day cycle. The response of WT (parental) tumors is included on the graph for comparison. Data shown are mean ± standard error (n = 10).

Treatment-Emergent Mutations in *NAEβ* Are Observed in AML and DLBCL Xenografts

MLN4924 has shown clinical activity in patients with AML (Wang et al., 2011). Therefore, we utilized THP-1 cells, a relevant subcutaneous AML preclinical model, to determine whether resistance to MLN4924 could be driven by *NAEβ* mutations. The subcutaneous model was utilized to facilitate harvesting tumors for subsequent analysis. On a clinically relevant schedule, MLN4924 was administered to SCID mice bearing THP-1 xenografts (90 mg/kg BID, twice-weekly), and uniform tumor regressions were observed (Figure 4A). Six of ten THP-1 xenografts regrew during the MLN4924 treatment period and were harvested for analysis. Three of these THP-1 xenografts contained a heterozygous mutation in *NAEβ* at A171T, one contained a heterozygous mutation at N209D, and the remaining two were wild-type for NAEβ so may be refractory through an alternate mechanism (Figure 4A and Table S2). Again, no mutations were observed in *NAE1*, *COPS5*, *UBC12*, or *NEDD8*. One A171T THP-1 xenograft was successfully re-established in SCID mice and shown to be resistant to MLN4924 when dosed at 90 mg/kg BID twice-weekly (Figure 4B). Pharmacodynamic evaluation in THP-1 A171T xenografts showed that MLN4924 produced minimal inhibition of NEDD8-cullin levels (Figures 4C and S5A), resulting in a reduced elevation of the CRL substrate pIκBα (Figures 4D and S5B) and a failure to activate apoptosis (Figures 4E and S5C) in comparison to THP-1 wild-type xenografts.

We have previously shown that activated B cell-like (ABC-) DLBCL may be particularly sensitive to MLN4924 through inhibition of constitutively active NF-κB signaling (Milhollen et al., 2010). To determine whether resistance to MLN4924 through *NAEβ* mutations occurs in models in which re-replication does not drive the terminal outcome, we followed OCI-Ly10 xenograft-bearing mice and administered MLN4924 (90 mg/kg BID, twice-weekly) for more than 100 days. Consistent with our previous findings, MLN4924 induced tumor regressions in the OCI-Ly10 model (Figure 4F). Only one of ten tumors regrew during therapy, and subsequent analysis revealed a heterozygous mutation in *NAEβ* at E204G. The tumor was re-implanted and was, as with the other re-introduced resistant tumors, resistant to MLN4924 treatment at 90 mg/kg BID (Figure 4G). These data demonstrate that, regardless of the MLN4924-dependent terminal outcome or genetic background, certain *NAEβ* mutations can drive resistance to MLN4924.

Mutations in the Nucleotide Binding Pocket and NEDD8 Binding Cleft of NAEβ Affect MLN4924 Adduct Formation and Dissociation from NAEβ

The *NAEβ* mutations that have been detected in MLN4924-resistant cells derived in tissue culture or in vivo occur in two areas of the gene, the nucleotide binding pocket at Alanine 171 and at various residues that are within or close to the NEDD8 binding cleft (Figures 5A and 5B). Mutations at Alanine 171 appear to be a "hotspot," since approximately two-thirds of the mutations detected lie at this residue (Figure 5A). Structural renderings of the A171T and A171D mutants suggest that decreased potency of MLN4924 could occur through a clash with the indane group of MLN4924 and the bulkier threonine or aspartic acid residue in mutant NAEβ (Figure 5B). In contrast, mutations found in the NEDD8 binding region of NAEβ are hypothesized to affect the affinity of NEDD8 and in turn the NEDD8-MLN4924 adduct (Figure 5B). To understand the biochemical consequences of mutations in these regions, recombinant enzymes expressing A171T, A171D, N209K, E204K, or G201V were constructed as representative of the two classes of mutations (Table 2). Structural modeling of A171T or A171D did not predict an effect on ATP binding, yet these mutations did result in weaker affinity for ATP. However, the titration profile and affinity for NEDD8 was largely unaffected by mutations to A171 (Table 2 and Figure S6). In contrast, mutations in the NEDD8 binding cleft (G201V and E204K) resulted in a shift in the NEDD8 titration profile, which attributes to a concomitant increase in the K_M for NEDD8 (Table 2 and Figure S6). Neither of these NEDD8 binding cleft mutations had much effect on the K_M for ATP. Interestingly, a mutation at G201V resulted in an increase in both the K_M for ATP and NEDD8, whereas the K_M for PPi was unaffected by any of these mutations (Table 2). In addition, other than the A171D mutant, the catalytic rate (k_{cat}) of the NAE reaction is not severely affected by any of these mutations; in fact, it appears that the G201V mutant is more catalytically active than is the wild-type enzyme (Table 2).

We have previously demonstrated that MLN4924 inhibits the NEDD8-NAEβ thioester form of NAE by occupying the nucleotide binding site and forming a covalent adduct between NEDD8 and MLN4924 (Brownell et al., 2010). To determine the effect of inhibitory potency of MLN4924 against wild-type and mutant enzymes, the PPi-ATP assay was performed using a concentration of 1 mM ATP. Interestingly, the A171T mutant was still capable of being inhibited by MLN4924 with only a modest 2-fold decrease in potency compared to wild-type enzyme (Table 2). MLN4924 did not inhibit A171D up to a concentration of 100 μM, suggesting that the bulkier aspartic acid residue impedes MLN4924 binding in the nucleotide binding pocket. MLN4924 was approximately 10-fold less active against the NEDD8 binding cleft mutants compared to wild-type enzyme. Compound 1, a structurally similar N6-substituted adenosine sulfamate, was used for comparison with MLN4924 (Brownell et al., 2010). The potency of Compound 1 decreased 7-fold versus the A171T mutant and 17,000-fold versus the A171D mutant (Table 2). A noticeable decrease in potency was

(C–E) CB.17 SCID mice bearing THP-1 parental or A171T xenografts were administered a single dose of MLN4924 90 mg/kg and tumors were excised at the indicated times and measured for (C) NEDD8-cullin conjugate levels by western blotting; (D) pIκBα levels by western blotting; and (E) cleaved caspase-3 levels by immunohistochemistry. Data shown are mean ± standard deviation (n = 3 replicates). (F) CB.17 SCID mice bearing OCI-Ly10 DLBCL xenografts were administered MLN4924 90 mg/kg BID on days 1, 4, 8, 11, 15, and 18 of a 21-day cycle for up to five cycles. Tumors were harvested at the end of treatment for analysis, and the mutational status of *NAEβ* was determined. Data shown are mean ± standard error (n = 10) for vehicle group.
(G) A tumor containing a glutamic acid 204 to glycine mutation was re-established in CB.17 SCID mice and treated with MLN4924 90 mg/kg BID on days 1, 4, 8, 11, 15, and 18 of a 21-day cycle. The response of WT (parental) tumors is included on the graph for comparison. Data shown are mean ± standard error (n = 10). See also Table S2 and Figure S5.

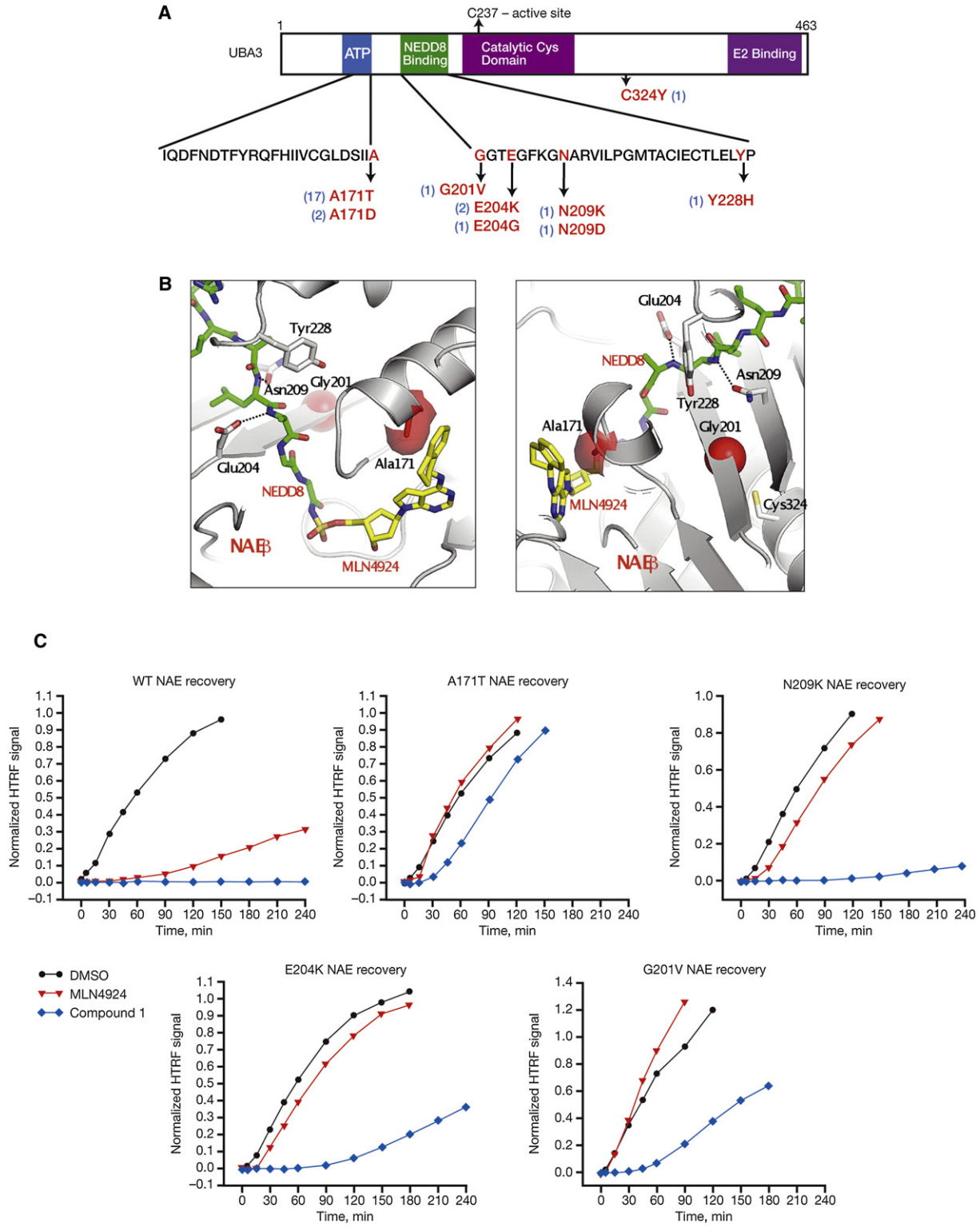

Figure 5. NAEβ Mutants Located in ATP Binding Pocket and NEDD8-Binding Cleft Lead to Faster Recovery from Enzyme Inhibition

(A) Schematic representation of location and frequency of NAEβ mutations detected in cells and xenografts.

(B) Crystal structure of NAE with NEDD8-MLN4924 adduct bound (PDB entry 3GZN; Brownell et al., 2010), highlighting NAEβ mutations.

(C) NAEβ mutants were inhibited with MLN4294 or compound 1 and purified, and complexes were added to transthiolation reaction containing 1 mM ATP to measure recovery of enzyme activity. Data shown are the mean of four replicates. See also Table S3.

Table 2. Biochemical Characterization of NAEβ Mutants.

NAEβ Enzyme	K_M ATP (μM)	K_M NEDD8 (μM)	K_M PPi (μM)	k_{cat} (s^{-1})	MLN4924 IC_{50} (μM)	Compound 1 IC_{50} (μM)
WT	88 ± 3	0.044 ± 0.024	22 ± 2	1.2 ± 0.2	0.049 ± 0.011	0.0041 ± 0.0002
A171T	600 ± 30	0.080 ± 0.018	22 ± 2	1.5 ± 0.4	0.10 ± 0.026	0.030 ± 0.002
A171D	1,900 ± 20	0.016 ± 0.0037	10 ± 2	0.33 ± 0.08	>100	70 ± 20
N209K	31 ± 1	0.43 ± 0.081	24 ± 2	2.0 ± 0.1	0.78 ± 0.16	0.076 ± 0.005
E204K	21 ± 1	0.48 ± 0.053	18 ± 1	1.3 ± 0.5	1.6 ± 0.20	0.17 ± 0.005
G201V	820 ± 36	3.5 ± 0.22	10 ± 1	3.7 ± 0.5	0.51 ± 0.057	0.0057 ± 0.0006

Several NAEβ mutants were characterized in the pyrophosphate exchange assay and analyzed for parameters of K_M for ATP, NEDD8, PPi, and catalytic activity. The K_M for each substrate was determined by titrating each substrate into the PPi-ATP assay and fitting the average of three replicates to the standard Michaelis-Menten equation, $y = V_{max}^{*}[S] / K_M + [S]$, where y is PPi-ATP activity. The standard error was extrapolated from the fit. The k_{cat} for each enzyme using three replicates was determined under optimal conditions (saturating ATP, PPi, and peak [NEDD8]) and using an [α-32P]-ATP standard curve. Each k_{cat} value represents the average and standard deviations of duplicates experiments. NAEβ mutants were tested in the pyrophosphate exchange using 1 mM ATP and measured for potency with MLN4924 and Compound 1. IC_{50} curves using the average of three replicates were fit using a sigmoidal logistics 3-parameter equation, $y = a / (1+([I]/IC_{50})^{b}$, where y is % inhibition, a is amplitude, and b is hill slope. Each IC_{50} value represents the average and standard deviations of duplicate experiments. See also Figure S6.

also observed with Compound 1 in the NEDD8 binding pocket mutants.

Since in vitro IC_{50}s of enzyme inhibition did not fully explain the resistance to MLN4924 observed, further compound characterization was performed to evaluate the rates of enzyme inactivation and the reversibility of compound inhibition. A171D NAEβ mutant was not used in these studies, because it was completely insensitive to MLN4924 inhibition. Enzyme-inhibitor complexes, NEDD8-MLN4924 or NEDD8-Compound 1, were pre-formed on the enzyme, purified, and added to a UBC12 transthiolation reaction to measure the recovery of enzyme activity (Figure 5C). As previously reported, NEDD8-MLN4924 was a tight-binding inhibitor of wild-type NAEβ with enzyme activity, recovering to approximately 30% of dimethylsulfoxide (DMSO) control levels by 240 min. In contrast, the recovery of enzymatic activity following MLN4924 inhibition was similar to that of the DMSO control for A171T, N209K, E204K, and G201V mutants. These data indicate that although the NEDD8-MLN4924 adduct is formed by the mutant enzymes, it is no longer a tight-binding inhibitor. The NEDD8-Compound 1 adduct binds more tightly to wild-type NAEβ than the NEDD8-MLN4924 adduct, with no discernible recovery of enzymatic activity at 240 min (Figure 5C). In addition, the NEDD8-Compound 1 adduct appears to be a tighter binder of all mutant NAE enzymes, suggesting that Compound 1 may be a more potent inhibitor of mutant enzyme in cells compared to MLN4924.

The rate of enzyme inactivation by MLN4924 for both A171T and N209K mutants was also dramatically slower compared to wild-type as opposed to Compound 1, for which the rate of wild-type and mutant enzyme inactivation was more rapid than MLN4924 (Table S3). These data provide a rationale for explaining the resistance that is conferred by mutations in *NAEβ*, namely, the slower rate of inactivation and faster off-rate of the NEDD8-MLN4294 adduct.

Cells Containing Mutations in NAEβ Form Lower Levels of NEDD8-MLN4924 Adduct and Show Increased Recovery of Pathway Activity

HCT-116 mutant cells lines (A171T and G201V) were evaluated during and after MLN4924 treatment to determine the effect of these mutations on pathway activity recovery. Cells were treated with MLN4924 10 μM for 1 hr, after which compound was removed and replaced with drug-free media; cells were harvested at 0 min, 15 min, 2 hr, or 5 hr postdrug washout (Figure 6A). In agreement with previous observations (Brownell et al., 2010), western blot analysis of wild-type cells indicated incomplete recovery of NEDD8-cullin and NEDD8-UBC12 and a persistence of NEDD8-MLN4924 adduct levels at both 1 μM and 10 μM for at least 5 hr postwashout. The prolonged pathway inhibition in the washout setting was corroborated by continued elevation of two CRL substrates, NRF2 and CDT1. In contrast, both A171T and G201V mutant cell lines showed almost-complete recovery of pathway activity as early as 15 min postwashout (Figure 6A). Interestingly, it appeared that the two mutant cell lines contained a reduced amount of NEDD8-MLN4924 adduct compared to wild-type cells, even though the levels of total NAEβ appeared similar. This would support the biochemical findings of a slower rate of adduct formation and weaker binding of adduct in the mutant enzymes.

To determine whether lower amounts of NEDD8-MLN4924 adduct were bound to NAEβ, cells were treated under the same washout conditions but subjected to immunoprecipitation assays with NAEβ (Figure 6B). Similar levels of NAEβ and NAE1 were detected in immunoprecipitates, indicating that the NAE heterodimer had been efficiently extracted from cell lysates. Immunoprecipitates were next probed with the NEDD8-MLN4924 antibody, which detected lower levels bound to A171T and G201V mutants compared to the wild-type enzyme. Lower levels of bound NEDD8-MLN4924 adduct in A171T and G201V mutants compared to wild-type enzyme were confirmed by running the 1 hr incubation samples on the same gel (Figure S7). It is likely that the amount of NEDD8-MLN4294 adduct bound to NAEβ is comprised mostly of an adduct bound to the wild-type but not the mutant enzyme, as the mutant enzyme can form an adduct but not bind the adduct tightly. To determine if higher levels of unbound adduct were present in mutant versus wild-type cells, the flow-through from the immunoprecipitates was probed with the NEDD8-MLN4924 adduct antibody (Figure 6B). However, there did not appear to be a difference in

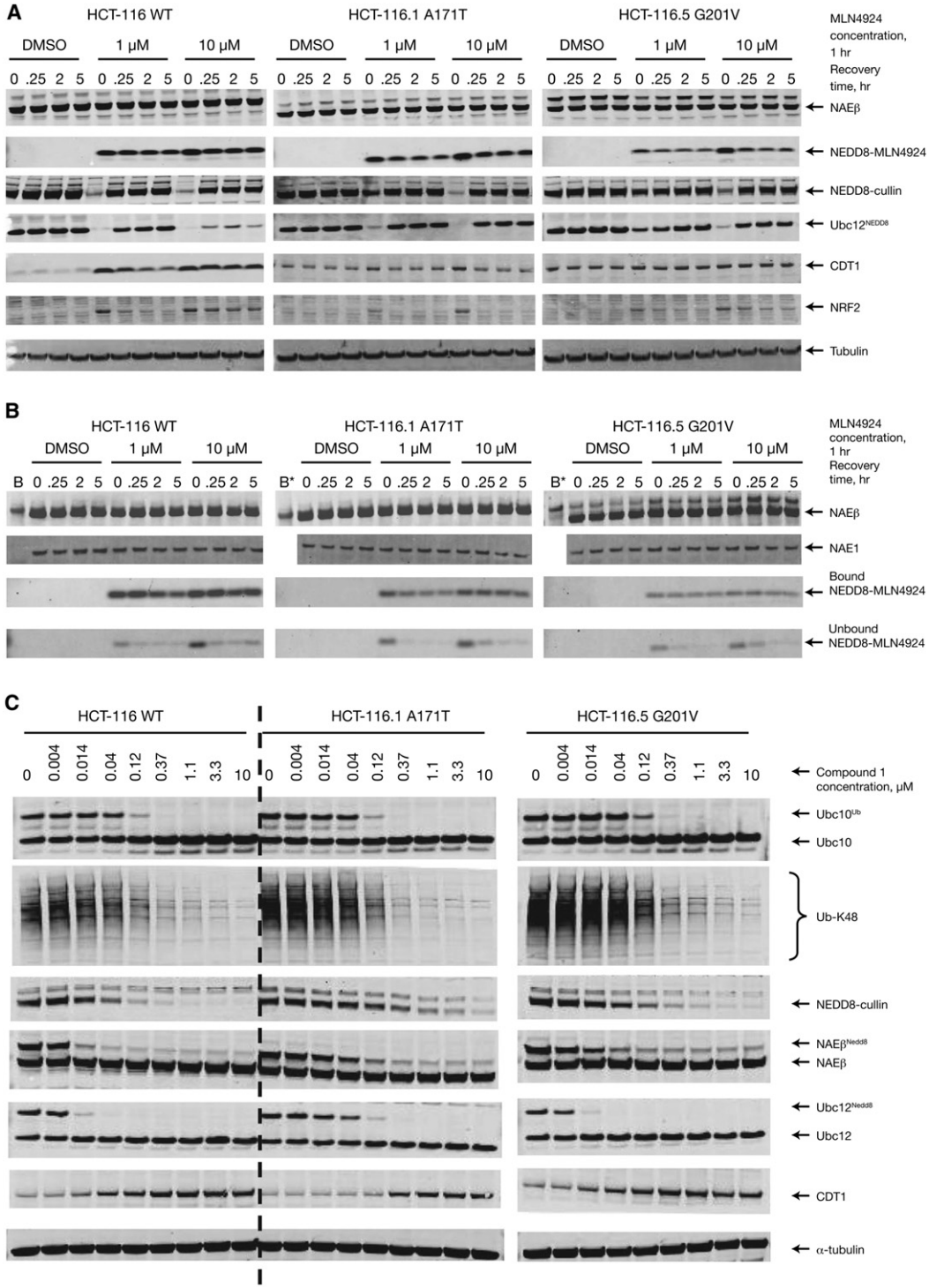

Figure 6. MLN4924-Resistant Cells with a Heterozygous *NAEβ* Mutation Show Reduced Levels of NEDD8-MLN4924 Adduct Formation, Faster Recovery of Pathway Inhibition, and Are More Sensitive to a Tighter-Binding NAE Inhibitor

(A) HCT-116 WT, A171T, or G201V cells were treated with MLN4924 1 μM or 10 μM for 1 hr, the compound was washed out, and the cells were incubated in drug-free media and harvested at the indicated times. Protein lysates were probed by western blotting for NEDD8-cullin, NEDD8-NAEβ, NEDD8-UBC12, NEDD8-MLN4924 adduct, CDT1, NRF2, and tubulin.

(B) Immunoprecipitation assays were performed with a NAEβ antibody and resultant isolates probed with NAEβ, NAE1, and NEDD8-MLN4924 adduct antibody. Flow through from the immunoprecipitation assays was probed with NEDD8-MLN4924 adduct antibody. See also Figure S7.

(C) HCT-116 WT, A171T, or G201V cells were treated with various concentrations of compound 1 for 4 hr, and protein lysates were probed by western blotting for UBC10, ubiquitin K48 chains, NEDD8-cullin, NEDD8-NAEβ, NEDD8-UBC12, CDT1, and α-tubulin.

the amount of free adduct in mutant versus wild-type cells, which may be due to proteolysis of adduct when it is released from NAEβ in cells. These data show that, following inhibition of mutant NAEβ in cells, pathway activity recovers quickly and correlates with lower amounts of NEDD8-MLN4924 adduct bound to the enzyme.

The data in biochemical and cell-based assays would suggest that a NEDD8-inhibitor adduct, which was able to bind more tightly to the enzyme, may overcome resistance to MLN4924 treatment-emergent NAE mutations. To test this hypothesis we used Compound 1, which in biochemical assays had faster rates of enzyme inhibition and slower rates of recovery compared to MLN4924. HCT-116 wild-type, and A171T and G201V mutant cells were exposed to increasing concentrations of Compound 1 for 4 hr and assessed for pathway activity by western blotting (Figure 6C). Since Compound 1 also inhibits UBA1, we could show comparable inhibition of ubiquitination of Ubc10 (an E2 for ubiquitin) and polyubiquitination in all cells (Figure 6C). In contrast to MLN4924 (see Figure 2), Compound 1 was able to produce comparable inhibition of NAEβ-NEDD8, NEDD8-cullin, and NEDD8-UBC12 in G201V mutant versus wild-type cells, and there was only a modest decrease in A171T mutant cells compared to wild-type cells. This likely reflects the quicker recovery of enzyme activity seen with Compound 1 in A171T biochemical assays. These data suggest that NEDD8-inhibitor compounds with improved binding affinities may overcome the resistance observed in the NAEβ mutations we have identified. In addition, to provide complete inhibition of the A171T mutation, alternative strategies may need to be employed, which could include the generation of covalent inhibitors of the enzyme.

Sequencing of DNA from AML, Colon Cancer, and Melanoma Tumor Samples Does Not Detect Preexisting Mutations in *NAEβ*

To determine whether mutations in *NAEβ* could be detected in cancer patients and therefore may exist prior to MLN4924 therapy, DNA from 50 colon cancer and melanoma tumor samples and 41 AML samples were subjected to Sanger and mass spectrometry-based (Sequenom platform) sequencing (Table S4). No *NAEβ* mutations were detected by either method, with the Sequenom platform having a sensitivity limit of approximately 10%. To increase the sensitivity of detection we subjected 21 of the AML samples to next-generation sequencing of *NAEβ* using the illumina platform but did not detect any mutations in *NAEβ*. Similarly, "preexisiting" mutations in *NAEβ* were not detected in wild-type HCT-116, Calu-6, and NCI-H460 cells by next-generation sequencing. Interestingly, one heterozygous *NAEβ* mutation (C249Y resulting from an amino acid change G > A) has been reported in an ovarian cancer patient in the Catalogue of Somatic Mutations in Cancer (Cosmic) database (total 218 tumor samples tested; http://www.sanger.ac.uk/perl/genetics/CGP/cosmic?action = bygene&ln = UBA3&start = 1&end = 1392&coords = AA%3Abp). This mutation is in a region of NAEβ that binds NAE1 (Walden et al., 2003) and so may interfere with heterodimer formation and enzyme activity. Thus, we were not able to detect a preexisting mutation in *NAEβ* in DNA isolated from patient tumors, leukemic blasts, or cancer cell lines.

DISCUSSION

MLN4924, a small-molecule inhibitor of an E1-activating enzyme (NAE) that is being tested as a cancer therapy in humans, has shown clinical activity with reports of complete responses in patients with AML (Wang et al., 2011). In this report we sought to characterize potential mechanisms of resistance to MLN4924 in preclinical models of cancer. We demonstrated that human tumor cell lines and xenografts grown in immunocompromised rodents can acquire resistance to MLN4924 through coding sequence mutations in *NAEβ*. These studies reveal a potential strategy for designing second-generation inhibitors that could overcome resistance mediated by mutations in *NAEβ*.

The occurrence of amino acid substitutions has been described as a common form of resistance for cancer drugs, such as tyrosine kinase inhibitors, including imatinib, gefitinib, and erlotinib (Shah et al., 2002; Kobayashi et al., 2005; Pao et al., 2005). More recent examples include amino acid substitutions in the anaplastic lymphoma kinase (ALK) following crizotinib therapy that occurred in lung cancer patients harboring an *EML4-ALK* translocation (Choi et al., 2010). Mutations in *ALK* that reduced sensitivity to crizotinib were originally described in preclinical studies using models of *NPM-ALK* translocations, which led to the studies' predictions that the mutations may occur in *EML4-ALK* cancers (Lu et al., 2009). These data demonstrate two important points: confirmation that the enzyme targets of these drugs "drive" the cancer, and that the activity of the inhibitors is through inhibition of the target. Furthermore, these observations have led to treatment paradigms that include retreating relapsed patients with a second-generation inhibitor that can target enzymes with amino acid substitutions (Cortes et al., 2011). This approach may be useful for NAEβ amino acid substitutions that are mechanisms of resistance to MLN4924 in clinical studies.

Treatment-emergent mutations in *NAEβ* were detected in the ATP binding pocket and NEDD8 binding cleft with approximately two-thirds at Alanine 171, representing a potential hotspot. Though mutations in both areas generally led to changes in affinities for ATP or NEDD8, this did not lead to a dramatic change in catalytic rate of NAE (except in the case of A171D and G201V). However, mutations in both areas of NAEβ led to a slower rate of enzyme inhibition and a NEDD8-MLN4924 adduct that was no longer tightly bound. We have previously demonstrated that NEDD8-MLN4924 adduct formation is necessary for potent NAE inhibition by MLN4924 and the tight binding nature of the adduct is required for in vitro and cellular potency (Brownell et al., 2010). In keeping with this notion, we demonstrated reduced pathway inhibition in cells and a more rapid recovery from compound inhibition in cell washout experiments. We used a nonselective E1 inhibitor (Compound 1) to probe the effects of more potent enzyme inhibition in vitro and in cells. Compound 1 forms an adduct with NEDD8 in vitro and shows a slower rate of recovery from enzyme inhibition compared to MLN4924 in the wild-type and mutant enzymes tested. These data indicate that the NEDD8-Compound 1 adduct is a tighter binder of wild-type and mutant NAEβ enzymes compared to MLN4924. Indeed, in A171T and G201V mutant HCT-116 cells Compound 1 was able to more potently inhibit

NEDD8-cullin and NEDD8-UBC12 thioester levels than did MLN4924. However, pathway inhibition in the A171T mutant HCT-116 cells was less pronounced than in the G201V mutant HCT-116 cells, which may indicate the need for a tighter binding inhibitor or a molecule capable of covalent inactivation of the A171T mutant. Nevertheless, these data support our notion that a NAE-selective, NEDD8-compound adduct with high affinity for mutant and wild-type enzymes should overcome resistance in cells and tumor xenografts. Unfortunately, it was not possible to test this in cell viability or xenograft experiments, as Compound 1 is nonselective for other E1 enzymes whose inhibition can result in viability effects (Brownell et al., 2010). It will be of interest to complete a thorough characterization of all *NAEβ* mutants and the mechanism by which they are conferring resistance to MLN4924. For example, the Y228H mutation corresponds with a residue previously shown to be important for "clamping" the C-terminus of NEDD8 into the adenylation domain, and the mutation of Y228 has been previously shown to diminish NEDD8 adenylation (Walden et al., 2003). This would suggest that this mutant enzyme is inefficient for NEDD8-activation. In addition, the mutation detected at C324Y is in a region of NAEβ that may also impact NEDD8 binding through structural perturbation of the NEDD8 binding cleft (see Figure 5B). Interestingly, Alanine at position 171 is conserved in most E1-activating enzymes, including UBA1, UBA6, and Sumo-activating enzyme, suggesting that selective inhibitors of these enzymes that are potential drug targets may also be susceptible to the same resistance mechanism.

The resistant cell lines were selected following a short exposure (four days) to high concentrations of MLN4924. All cell lines were isolated as clonal populations, shown to be resistant to MLN4924 and still sensitive to other chemotherapies, including proteasome inhibition (bortezomib), an anthracycline (doxorubicin), and a topoisomerase I inhibitor (SN-38). Reverse transcription-polymerase chain reaction analysis of the clones indicated an elevation of drug efflux mechanisms with increased detection of mRNA for Pgp and BCRP in some cell lines. However, it appears that the elevation of drug efflux does not significantly contribute to the resistance, as cotreating cells with a number of Pgp, BCRP, and MRP2 inhibitors did not sensitize cells to MLN4924 (dipyridamole, Shalinsky et al., 1993; MK519, Gekeler et al., 1995; GF120918, Hyafil et al., 1993; K0143, Allen et al., 2002; LY5979, Dantzig et al., 1996). These data, in addition to the presence of mutations in NAEβ, indicate that the resistance is driven by mutations in the target enzyme.

MLN4924 induces DNA damage in cells via re-replication (Milhollen et al., 2011), and this mechanism of inducing hyperreplication of DNA may aid in the development of resistance through increased random mutagenesis. HCT-116, H460, and Calu-6 cells all undergo DNA re-replication, whereas OCI-Ly10 cells do not (Milhollen et al., 2010). We were able to detect an *NAEβ* mutation in the OCI-Ly10 model, suggesting that resistant mutants can emerge irrespective of the mechanism of action of MLN4924. Interestingly, HCT-116 cells have a deficiency in the DNA mismatch repair protein MLH1 (Taverna et al., 2000), and this may make them more susceptible to resistance mutations by virtue of increased genomic instability. This assertion may be supported by the increased number of mutations detected in HCT-116 cell lines and xenografts compared to others used in these studies that do not possess the same defect in DNA repair. It will be of interest to understand whether the mechanism of DNA re-replication and/or defects in DNA repair make cells more likely to develop resistance to MLN4924 through mutations in *NAEβ*.

In these studies we have detected heterozygous mutations in *NAEβ*, where cells maintain one wild-type copy of *NAEβ*. An important model system to conclusively prove that mutations in *NAEβ* drive resistance would be an engineered cell line that only expresses the mutant, not the wild-type, enzyme. Thus far, we have not been successful in developing such a model system. It is possible that a wild-type enzyme is required to support growth and that the role of the mutant enzyme is to enable NEDD8 conjugation when the wild-type enzyme is under transient inhibition by MLN4924 in cells and xenografts. Since the mutation frequency of *NAEβ* in cell and xenograft populations is ~50%, we developed mass spectrometry and next-generation sequencing methodologies that allowed us to detect *NAEβ* mutations to a frequency of ~0.5%. We were not able to detect mutations in *NAEβ* that were preexisting in the cell line, xenograft, or patient tumor DNA samples, suggesting that the mutations are acquired during the selection process. A search of single-nucleotide polymorphism databases did not reveal the existence of the mutations reported in human populations, but we cannot rule out the possibility that mutations do exist at a lower frequency than 0.5% in tumors. Indeed, a mutation in *NAEβ* has been reported in the Cosmic database in an ovarian cancer sample at C249Y. This residue is in a region of NAEβ that is involved in binding NAE1 (Walden et al., 2003), and so it is possible that this would interfere with heterodimer formation and enzyme activity. It will be important to continue efforts to establish whether mutations are preexisiting, as this may predict patients who are more likely to relapse following MLN4924 administration.

These studies demonstrate that treatment-emergent mutations in *NAEβ* can confer resistance to MLN4924 in preclinical models. Since *NAEβ* mutations appear to be the most common cause of resistance in our studies, irrespective of the cellular outcome following NAE inhibition, this confirms the selectivity of MLN4924 for its target. We did observe the regrowth of THP-1 AML xenografts that did not contain a mutation in *NAEβ*, suggesting that other mechanisms of resistance to MLN4924 are also likely to occur. Mechanisms of MLN4924 resistance will be explored further so that continued clinical strategies can be employed in responding patients. These may take the form of combination partners based on complimentary biology in the context of NAE inhibition or next-generation NAE inhibitors targeted to mutant NAEβ that may emerge in MLN4924-relapsed patients.

EXPERIMENTAL PROCEDURES

Materials

[32P]-PPi (Cat. No. NEX019), [α-32P]-ATP (Cat. No. BLU003H250UC), and [α-32P]-ATP (Cat. No.BLU002250UC) were obtained from Perkin Elmer (Boston, MA, USA). Other chemicals were purchased from Sigma-Aldrich (St. Louis, MO, USA). N-terminal FLAG-tagged NEDD8 with the sequence of N-MDYKDDDDK-NEDD8 was expressed and purified as described (Soucy

et al., 2009a). Untagged NEDD8 and N15- and C13-labeled, untagged NEDD8 (NEDD8*) was expressed and purified similarly. N-terminal GST-tagged Ubc12 was expressed and purified as described (Soucy et al., 2009a). His-tagged NAE proteins (*NAE1* and His-tagged *NAEβ* wild-type and mutants) were cloned into Rosetta (DE3) cells and complexes were generated by co-expression into *Escherichia coli*. Expressed proteins were purified by affinity (Ni-NTA agarose; Qiagen, Valencia, CA, USA) or conventional chromatography. GST-tagged NAE proteins (NAE1 and GST-tagged NAEβ wild-type and mutants) were generated by co-infection of Sf9 cells (Soucy et al., 2009a). GST-NAE proteins were purified by affinity chromatography (Glutathione Sepharose 4B; GE Healthcare, Piscataway, NJ, USA) followed by Hi-Trap Q HP (GE Healthcare).

Cell Culture, Cell Viability, and Western Blot Analysis

Cell line cultures were maintained using the appropriate cell culture media as recommended by ATCC and as previously reported (Soucy et al., 2009a; Milhollen et al., 2010). To derive resistant cell lines HCT-116, Calu-6, and NCI-H460 cells were incubated with high concentrations of MLN4924 ($\geq EC_{90}$ concentrations) for four days, after which the remaining cells were removed, plated as single-cell clones, and cultured in drug-free media. Cell viability assays were completed using a 96 hr ATPlite assay (Perkin Elmer) as previously reported (Soucy et al., 2009a). Whole-cell extracts were prepared and immunoblotting assays performed as previously described (Soucy et al., 2009a) with primary antibodies as follows: CDT1, NRF2, NEDD8, NAEβ, UBC12, and MLN4924-NEDD8-ADS (MIL22; Millennium, Cambridge, MA, USA); UBC10 (Boston Biochem, Cambridge, MA, USA); K48 (Millipore, Billerica, MA, USA); NAE1 (Sigma-Aldrich); and tubulin (Santa Cruz, Santa Cruz, CA, USA). Secondary Alexa-680-labeled antibodies to rabbit/mouse IgG (Molecular Probes, Grand Island, NY, USA) were used as was appropriate, and blots were imaged using the Li-Cor Odyssey Infared Imaging system.

Cell Culture Washout and Immunoprecipitation Analysis

HCT-116 wild-type, A171, and G201V cells were treated with either MLN4924 1 μM or 10 μM or DMSO for 1 hr. Cells were washed with media to remove the drug, replaced with fresh media, and harvested at 0 hr, 0.25 hr, 2 hr, or 5 hr postwashout. Lysates were prepared as previously reported (Soucy et al., 2009a). Washout lysate (100 μg) was incubated with 5 μg NAEβ antibody on ice for 1 hr. Slurry Protein G agarose (Upstate, Billerica, MA, USA; 50 μl of 50%) was added and tumbled for 1 hr at 4°C. Samples were spun down and supernatant removed to fresh tube (unbound fraction), and beads were washed three times with buffer. Sample buffer (50 μl 2X) was added to beads (bound fraction), and samples were fractionated on sodium dodecyl sulfate polyacrylamide gel electrophoresis gels and immunobloted as indicated. For the unbound fraction, the above procedure was repeated using 2 μg MLN4924-NEDD8-ADS (MIL22) antibody and 50 μl of 50% slurry Protein A agarose (Pierce, Rockford, IL, USA).

Immunocompromised Rat and Mouse Antitumor Studies

Female NCr nude rats (Taconic Farms, Germantown, NY, USA), aged 6–8 weeks, were inoculated with 10×10^6. HCT-116 cells were subcutaneously injected in the right flank. Tumor growth was measured using digital vernier calipers. When mean tumor growth reached ~500 mm^3, rats were assigned randomly to treatment groups and dosed subcutaneou sly with vehicle (20% hydroxypropyl-beta-cyclodextrin) or MLN4924. Rats received one dose per day twice-weekly for two weeks (days 1, 4, 8, and 11) of a 21-day therapy cycle. After three cycles of treatment, refractory tumors were collected. Female CB-17 SCID mice (Charles River Laboratories, Wilmington, MA, USA), aged 6–8 weeks, were inoculated with 2×10^6 THP-1 or OCI-Ly10 cells with Matrigel support (1:1, v/v). When mean tumor growth reached 200 mm^3, mice were assigned randomly to treatment groups and dosed subcutaneously with vehicle (20% hydroxypropyl-beta-cyclodextrin) or MLN4924. Mice received two doses per day twice-weekly (days 1, 4, 8, 11, 15, 18, 22, and so on) until tumors reached ~500–800 mm^3. Tumors were then collected and one 40 mg–50 mg piece of tumor was subcutaneously implanted using a 13-gauge trocar needle into 6–8 naive animals for further study. In addition, tumor DNA was extracted for mutational analysis as described in the Supplemental Experimental Procedures. All studies were done in accordance with the standards of ethical treatment approved by the Institutional Animal Care and Use Committee (IACUC) and Association for the Assessment and Accreditation of Laboratory Animal Care (AAALAC). All animal experiments were approved by the Institutional Animal Care and Use Committee of Millennium Pharmaceuticals Inc.

Pharmacodynamic Marker Analysis

Mice and rats bearing HCT-116, THP-1, or OCI-Ly10 tumors were administered a single MLN4924 dose, and at the indicated times, tumors were excised and extracts prepared. The relative levels of NEDD8-cullin and plκBα were estimated by quantitative immunoblot analysis (Li-Cor Odyssey system) using Alexa680-labeled anti-IgG (Molecular Probes) as the secondary antibody. For the analysis of CDT1 and cleaved caspase-3 levels in tumor sections, formalin-fixed, paraffin-embedded tumor sections were stained with the relevant antibodies, amplified with HRP-labeled secondary antibodies, and detected with the ChromoMap DAB Kit (Ventana Medical Systems, Tuscon, AZ, USA). Slides were counterstained with hematoxylin. Images were captured using an Eclipse E800 microscope (Nikon Instruments, Melville, NY, USA) and Retiga EXi color digital camera (QImaging, Surrey, BC, Canada) and processed using Metamorph software (Molecular Devices, Sunnyvale, CA, USA). CDT1 and cleaved caspase-3 are expressed as a function of the DAB signal area.

Measurement of NEDD8-MLN4924 Adduct Levels in Tumor Xenografts

To quantify the absolute level of NEDD8-MLN4924 adduct in tumor xenografts, 30 μg total protein of each lysate sample was mixed with 0.1 pmol (0.9 ng) NEDD8*-MLN4924 followed by NuPAGE Bis-Tris 4%–12% SDS gel separation (Invitrogen); NEDD8 gel fractions were excised and in-gel tryptic digestion was performed as described previously (Brownell et al., 2010). The digests were analyzed on an LC/MS/MS system (Brownell et al., 2010). The NEDD8-MLN4924 adduct amount in each sample was calculated from the ratio of the peak areas of Gly-Gly-MLN4924 to Gly*-Gly*-MLN4924 in the chromatogram.

Biochemical Characterization of NAEβ and Mutant Enzymes

Biochemical characterization and IC_{50} determinations were performed using an improved pyrophosphate exchange assay developed by Bruzzese et al. (2009). ATP-PPi exchange reactions were performed in buffer containing 50 mM HEPES (pH 7.5), 25 mM NaCl, 10 mM $MgCl_2$, 0.05% BSA, 0.01% Tween-20, and 1 mM DTT. NEDD8 titrations were performed by serial dilution of NEDD8 into a 96-well assay plate containing 10 nM NAE, 1 mM ATP, and 0.2 mM PPi (50 cpm/pmol [32P] PPi). Assays were incubated for 30 min at 37°C in a final volume of 50 μl and were stopped with the addition of 500 μl of 5% (w/v) trichloroacetic acid containing 10 mM PPi. The quenched reactions were transferred to a dot-blot apparatus fitted with activated charcoal filter paper as described previously (Bruzzese et al., 2009). CPM was converted to pM/min using an [α-P32] ATP standard curve. Since NEDD8 was inhibitory at higher concentrations for wild-type and A171T/D NAEβ, inhibited top points for these particular mutants were excluded before fitting for an estimated K_M. All K_Ms were fit using the standard Michaelis-Menten equation for enzyme kinetics. ATP K_Ms were determined by serial diluting ATP into a 96-well assay plate under similar assay conditions. Reactions were initiated with addition of NEDD8 (0.16 μM for wild-type, A171T/D and 2.5 μM for N209K, E204K, and G201V). Assays were incubated for 30 min at 37°C. PPi titrations were performed under similar conditions, except with serial dilution of PPi instead and using 1 mM ATP.

IC_{50}s were determines by serial dilution of each compound into a 96-well assay plate containing 5 nM NAE, 1 mM ATP, and 0.2 mM PPi (50 cpm/pmol [32P] PPi). Reactions were initiated with addition of NEDD8 (0.16 μM for wild-type, A171T/D, and 2.5 μM for N209K, E204K, and G201V). Assays were incubated for 60 min at 37°C in a final volume of 50 μl and were stopped as previously described.

The enzyme reversibility assay was run in the FLAG-NEDD8-GST-UBC12 HTRF transthiolation assay described previously (Soucy et al., 2009a; Brownell et al., 2010). Final concentrations of each enzyme after dilution were 10 pM wild-type NAEβ, 12.5 pM A171T NAEβ, 30 pM N209K NAEβ, and 33 pM E204K/G201V NAEβ.

Clinical Human Tumor Testing

All human tumor samples were obtained from commercial vendors (Supplemental Experimental Procedures) and were de-identified prior to purchase and analysis.

AML

Forty one unique malignant AML patient tumors (21 bone marrow aspirates and 20 bone marrow mononuclear cells) were genotyped for mutations found in preclinical models using the sequenom NAEβ assays (Supplemental Experimental Procedures), and the full gene was sequenced by an Illumina Next-Generation sequencing assay. All samples were found to be wild-type for NAEβ. The AML tumors represented newly diagnosed and relapsed patients with M1-M5 diagnosis classification. The blast tumor count ranged from 2% to 94%. Matched peripheral blood mononuclear cells were also sequenced and found to be wild-type.

Colon Cancer

A collection of 50 unique mucinous and sigmoidal colon adenocarcinomas with representative histologies of poor, moderate, and well-differentiated and 10% to 100% tumor per tissue were genotyped for mutations found in preclinical models using the Sequenom NAEβ assays, and the full gene was sequenced by Sanger sequencing. All samples were found to be wild-type for NAEβ.

Melanoma

A collection of 25 unique epithelioid and spindle cell-type melanoma adenocarcinomas, ranging from 25% to 100% tumor per tissue, were genotyped for mutations found in preclinical models using the Sequenom NAEβ assays, and the full gene was sequenced by Sanger sequencing. All samples were found to be wild-type for NAEβ.

SUPPLEMENTAL INFORMATION

Supplemental Information includes seven figures, four tables, and Supplemental Experimental Procedures and can be found with this article online at doi:10.1016/j.ccr.2012.02.009.

ACKNOWLEDGMENTS

All authors were employees of Millennium Pharmaceuticals, Inc., at the time of this work. Millennium Pharmaceuticals, Inc., is developing MLN4924.

Received: October 5, 2011
Revised: December 12, 2011
Accepted: February 6, 2012
Published: March 19, 2012

REFERENCES

Allen, J.D., van Loevezijn, A., Lakhai, J.M., van der Valk, M., van Tellingen, O., Reid, G., Schellens, J.H., Koomen, G.J., and Schinkel, A.H. (2002). Potent and specific inhibition of the breast cancer resistance protein multidrug transporter in vitro and in mouse intestine by a novel analogue of fumitremorgin C. Mol. Cancer Ther. *1*, 417–425.

Brownell, J.E., Sintchak, M.D., Gavin, J.M., Liao, H., Bruzzese, F.J., Bump, N.J., Soucy, T.A., Milhollen, M.A., Yang, X., Burkhardt, A.L., et al. (2010). Substrate-assisted inhibition of ubiquitin-like protein-activating enzymes: the NEDD8 E1 inhibitor MLN4924 forms a NEDD8-AMP mimetic in situ. Mol. Cell *37*, 102–111.

Bruzzese, F.J., Tsu, C.A., Ma, J., Loke, H.K., Wu, D., Li, Z., Tayber, O., and Dick, L.R. (2009). Development of a charcoal paper adenosine triphosphate: pyrophosphate exchange assay: kinetic characterization of NEDD8 activating enzyme. Anal. Biochem. *394*, 24–29.

Choi, Y.L., Soda, M., Yamashita, Y., Ueno, T., Takashima, J., Nakajima, T., Yatabe, Y., Takeuchi, K., Hamada, T., Haruta, H., et al; ALK Lung Cancer Study Group. (2010). EML4-ALK mutations in lung cancer that confer resistance to ALK inhibitors. N. Engl. J. Med. *363*, 1734–1739.

Cortes, J., Hochhaus, A., Hughes, T., and Kantarjian, H. (2011). Front-line and salvage therapies with tyrosine kinase inhibitors and other treatments in chronic myeloid leukemia. J. Clin. Oncol. *29*, 524–531.

Dantzig, A.H., Shepard, R.L., Cao, J., Law, K.L., Ehlhardt, W.J., Baughman, T.M., Bumol, T.F., and Starling, J.J. (1996). Reversal of P-glycoprotein-mediated multidrug resistance by a potent cyclopropyldibenzosuberane modulator, LY335979. Cancer Res. *56*, 4171–4179.

Gekeler, V., Ise, W., Sanders, K.H., Ulrich, W.R., and Beck, J. (1995). The leukotriene LTD4 receptor antagonist MK571 specifically modulates MRP associated multidrug resistance. Biochem. Biophys. Res. Commun. *208*, 345–352.

Hyafil, F., Vergely, C., Du Vignaud, P., and Grand-Perret, T. (1993). In vitro and in vivo reversal of multidrug resistance by GF120918, an acridonecarboxamide derivative. Cancer Res. *53*, 4595–4602.

Kobayashi, S., Boggon, T.J., Dayaram, T., Jänne, P.A., Kocher, O., Meyerson, M., Johnson, B.E., Eck, M.J., Tenen, D.G., and Halmos, B. (2005). EGFR mutation and resistance of non-small-cell lung cancer to gefitinib. N. Engl. J. Med. *352*, 786–792.

Lin, H.K., Chen, Z., Wang, G., Nardella, C., Lee, S.W., Chan, C.H., Yang, W.L., Wang, J., Egia, A., Nakayama, K.I., et al. (2010a). Skp2 targeting suppresses tumorigenesis by Arf-p53-independent cellular senescence. Nature *464*, 374–379.

Lin, J.J., Milhollen, M.A., Smith, P.G., Narayanan, U., and Dutta, A. (2010b). NEDD8-targeting drug MLN4924 elicits DNA rereplication by stabilizing Cdt1 in S phase, triggering checkpoint activation, apoptosis, and senescence in cancer cells. Cancer Res. *70*, 10310–10320.

Lu, L., Ghose, A.K., Quail, M.R., Albom, M.S., Durkin, J.T., Holskin, B.P., Angeles, T.S., Meyer, S.L., Ruggeri, B.A., and Cheng, M. (2009). ALK mutants in the kinase domain exhibit altered kinase activity and differential sensitivity to small molecule ALK inhibitors. Biochemistry *48*, 3600–3609.

Milhollen, M.A., Traore, T., Adams-Duffy, J., Thomas, M.P., Berger, A.J., Dang, L., Dick, L.R., Garnsey, J.J., Koenig, E., Langston, S.P., et al. (2010). MLN4924, a NEDD8-activating enzyme inhibitor, is active in diffuse large B-cell lymphoma models: rationale for treatment of NF-kappaB-dependent lymphoma. Blood *116*, 1515–1523.

Milhollen, M.A., Narayanan, U., Soucy, T.A., Veiby, P.O., Smith, P.G., and Amidon, B. (2011). Inhibition of NEDD8-activating enzyme induces rereplication and apoptosis in human tumor cells consistent with deregulating CDT1 turnover. Cancer Res. *71*, 3042–3051.

Nalepa, G., Rolfe, M., and Harper, J.W. (2006). Drug discovery in the ubiquitin-proteasome system. Nat. Rev. Drug Discov. *5*, 596–613.

Pao, W., Miller, V.A., Politi, K.A., Riely, G.J., Somwar, R., Zakowski, M.F., Kris, M.G., and Varmus, H. (2005). Acquired resistance of lung adenocarcinomas to gefitinib or erlotinib is associated with a second mutation in the EGFR kinase domain. PLoS Med. *2*, e73.

Sellers, W.R. (2011). A blueprint for advancing genetics-based cancer therapy. Cell *147*, 26–31.

Schulman, B.A., and Harper, J.W. (2009). Ubiquitin-like protein activation by E1 enzymes: the apex for downstream signalling pathways. Nat. Rev. Mol. Cell Biol. *10*, 319–331.

Shah, N.P., Nicoll, J.M., Nagar, B., Gorre, M.E., Paquette, R.L., Kuriyan, J., and Sawyers, C.L. (2002). Multiple BCR-ABL kinase domain mutations confer polyclonal resistance to the tyrosine kinase inhibitor imatinib (STI571) in chronic phase and blast crisis chronic myeloid leukemia. Cancer Cell *2*, 117–125.

Shalinsky, D.R., Jekunen, A.P., Alcaraz, J.E., Christen, R.D., Kim, S., Khatibi, S., and Howell, S.B. (1993). Regulation of initial vinblastine influx by P-glycoprotein. Br. J. Cancer *67*, 30–36.

Soucy, T.A., Smith, P.G., Milhollen, M.A., Berger, A.J., Gavin, J.M., Adhikari, S., Brownell, J.E., Burke, K.E., Cardin, D.P., Critchley, S., et al. (2009a). An inhibitor of NEDD8-activating enzyme as a new approach to treat cancer. Nature *458*, 732–736.

Soucy, T.A., Smith, P.G., and Rolfe, M. (2009b). Targeting NEDD8-activated cullin-RING ligases for the treatment of cancer. Clin. Cancer Res. *15*, 3912–3916.

Swords, R.T., Kelly, K.R., Smith, P.G., Garnsey, J.J., Mahalingam, D., Medina, E., Oberheu, K., Padmanabhan, S., O'Dwyer, M., Nawrocki, S.T., et al. (2010). Inhibition of NEDD8-activating enzyme: a novel approach for the treatment of acute myeloid leukemia. Blood *115*, 3796–3800.

Taverna, P., Liu, L., Hanson, A.J., Monks, A., and Gerson, S.L. (2000). Characterization of MLH1 and MSH2 DNA mismatch repair proteins in cell lines of the NCI anticancer drug screen. Cancer Chemother. Pharmacol. *46*, 507–516.

Walden, H., Podgorski, M.S., and Schulman, B.A. (2003). Insights into the ubiquitin transfer cascade from the structure of the activating enzyme for NEDD8. Nature *422*, 330–334.

Wang, M., Medeiros, B.C., Erba, H.P., DeAngelo, D.J., Giles, F.J., and Swords, R.T. (2011). Targeting protein neddylation: a novel therapeutic strategy for the treatment of cancer. Expert Opin. Ther. Targets *15*, 253–264.

Watson, I.R., Irwin, M.S., and Ohh, M. (2011). NEDD8 pathways in cancer, sine quibus non. Cancer Cell *19*, 168–176.